Synthesis of Abiotic Supramolecular Polymers Inside Living Cells via Organocatalysis-Mediated Self-Assembly

Wang, Hucheng; Zheng, Ya Ting; Zhang, Jiahao; Gao, Yuliang; Chen, Jingjing; Cai, Peiwen; van Esch, Jan H.; Li, Hui; Wang, Yiming; More Authors

DOI
10.1002/anie.202500998

Publication date
2025

Document Version
Final published version

Published in
Angewandte Chemie - International Edition

GDCh Research Article Angewandte International Edition Chemie www.angewandte.org

How to cite: *Angew. Chem. Int. Ed.* **2025**, *64*, e202500998
doi.org/10.1002/anie.202500998

Supramolecular Polymers **Hot Paper**

Synthesis of Abiotic Supramolecular Polymers Inside Living Cells via Organocatalysis-Mediated Self-Assembly

Hucheng Wang[+], Ya-Ting Zheng[+], Jiahao Zhang, Yuliang Gao, Jingjing Chen, Peiwen Cai, Junyou Wang, Jan H. van Esch, Xuhong Guo, Hui Li, and Yiming Wang**

Abstract: Cells execute mesmerizing functions using supramolecular polymers (SPs) formed through the self-assembly of biological precursors. Integration of the vast array of synthetic SPs with living cells would offer a powerful way to remold cellular functions and bridge the gap between synthetic materials and the biological realm, yet remains a challenge because of the lack of robust abiotic SP systems that can be triggered to self-assemble inside cells. Here, we report how fully abiotic SPs can be synthesized inside living cells via an organocatalysis-responsive self-assembly strategy, and how the in situ-generated SPs are capable of interfering and can interfere with cellular functions. The incorporation of a nucleophilic organocatalyst (**CAT**) into living cells accelerates the intracellular conversion of hydrazide (**H**) and aldehyde-derived precursors (**A**) to hydrazone-based monomers ($\mathbf{HA_3}$) that locally self-assemble into SPs. Interestingly, the in situ-generated SPs possess ignorable effects on cell viability and proliferation but remarkably hinder cell migration. Furthermore, the presence of SPs is found to retard intracellular diffusion and alter the organization of the actin cytoskeleton, both of which are suggested to be responsible for the hindered cellular migration. In considering the vastly wide range of synthetic SPs, tremendous non-natural cellular functionalities can be obtained by in situ-synthesizing SPs.

Introduction

Living cells have been identified as a complex supramolecular self-assembly system that executes many pivotal intracellular functions using supramolecular polymers (SPs) formed through the self-assembly of biological building blocks.[1,2] For instance, the self-assembly of tubulin into microtubules underpins signal transduction,[3] intracellular transportation,[4] and cell division.[5] As an inspiration, many abiotic SPs bearing diverse properties have been designed and synthesized in the lab. It is believed that integrating these manmade SPs with living cells would afford reinforced or completely new cellular functions and thus provide a promising approach to connect synthetic chemistry and the biological realm.[6]

Synthetic chemists have realized the self-assembly of peptide-based monomers inside living cells triggered by endogenous stimuli,[7,8] unlocking enticing applications in biomedicine.[9] For instance, by exploiting the overexpression of enzymes in cancer cells including alkaline phosphatase,[10,11] esterase,[12,13] protease,[14] and sulfatase,[15] the technique of enzyme-instructed self-assembly (EISA) has been developed,[16,17] leading to intracellular formation of peptide-based SPs for imaging and elimination of cancer cells.[18–20] Despite these advances, the intracellular self-assembly of bio-derived SPs in response to endogenous stimuli remains to face several inherent issues: 1) the limited diversity of natural precursors relative to fully synthetic counterparts compromises the range of functionalities; 2) the hydrolysis propensity of bio-derived SPs hinders long-term function; 3) the involved endogenous stimuli, in contrast to exogenous stimuli, are difficult to control. Very recently, some examples of intracellular self-assembly triggered by external photosignal were demonstrated, the monomers remain to be limited to bio-derived peptides.[21,22]

In recent years, intracellular synthesis of conventional covalent polymers has been realized by initiating the polymerization of small organic monomers inside living cells using free-radicals,[23–25] bioconjugate chemistry,[26,27] and endogenous redox reactions.[28,29] However, with respect to noncovalently featured SPs, covalent polymers are hard to degrade and are lacking dynamics that are vital to living

[*] H. Wang[+], J. Zhang, Y. Gao, J. Chen, P. Cai, J. Wang, X. Guo, Y. Wang
State Key Laboratory of Chemical Engineering, School of Chemical Engineering, East China University of Science and Technology, Shanghai 200237, P.R. China
E-mail: yimingwang@ecust.edu.cn

Y.-T. Zheng[+], H. Li
School of Systems Science and Institute of Nonequilibrium Systems, Beijing Normal University, Beijing 100875, P.R. China
E-mail: huili@bnu.edu.cn

J. H. van Esch
Department of Chemical Engineering, Delft University of Technology, Delft 2629 HZ, The Netherlands

H. Li
Key Laboratory of Cell Proliferation and Regulation Biology, Ministry of Education, Beijing Normal University, Beijing 100875, P.R. China

Y. Wang
Shanghai Key Laboratory for Intelligent Sensing and Detection Technology, East China University of Science and Technology, Shanghai 200237, P.R. China

[+] These authors contributed equally to this work.

Additional supporting information can be found online in the Supporting Information section

systems.[30] So far, to our best knowledge, imposing the synthesis of fully abiotic SPs inside living cells is rarely reported because of the lack of an appropriate stimuli-responsive self-assembly system, the realization of which would offer a lifelike and more controllable approach to remold intracellular functions.

Herein, we demonstrate how fully abiotic SPs can be synthesized inside living cells using an organocatalysis-mediated self-assembly strategy, and how the in situ-produced SPs can alter the intrinsic cellular behaviors. The living cells containing pre-installed nucleophilic organocatalyst are capable of catalyzing the intracellular formation and self-assembly of hydrazone-based small molecular monomers, giving rise to abiotic SPs inside the cells. Interestingly, these in situ-formed SPs are found to be compatible with the cells, without showing adverse effects on cell viability and proliferation. To our surprise, the cells containing the SPs exhibit hindered migration relative to normal cells. Further investigations suggest that the hindered cellular migration is ascribed to the fact that the generation of SPs restricts intracellular diffusion and interferes with the organization of the actin cytoskeleton. This work demonstrates that growing abiotic SPs inside living cells via a fully synthetic approach would possess potent potential to alter or enhance cellular functions in an unexpected way. Although Eelkema and colleagues also explored the intracellular formation of hydrazone-based SPs, their case is catalysis free and time consuming (overnight incubation), showing limited controllability. Additionally, the cells died after growing the SPs very likely caused by the use of high concentrations of the self-assembling reagents. More importantly, the biological effect of the SPs remains underexplored.[31]

Results and Discussion

To arrive at the synthesis of abiotic SPs in living cells, we proposed the following design rules: 1) the SPs can be triggered to self-assemble by exogenous stimuli, and all the involved molecules, including monomers and stimuli, are abiotic and should be nontoxic to living cells; 2) to ensure intracellular self-assembly, the monomers are required to possess a high self-assembly capability; 3) small molecular self-assembling building blocks and stimuli are preferred to realize an efficient cellular internalization and accumulation through passive diffusion.

To arrive at the proposed goal, a dynamic small molecular self-assembly system involving the catalytic formation and self-assembly of hydrazone-based monomers is employed. The monomers (**HA_3**) are formed from non-assembling hydrazide (**H**) and aldehyde (**A**) precursors via the formation of hydrazone bonds and self-assemble into one-dimensional SPs with a diameter of ~3.7 nm (Figure 1a–c and Figure S1). The addition of nucleophilic catalysts, including aniline and acid, can dramatically accelerate the formation and self-assembly of **HA_3**,[32] making the formation of the hydrazone-based SPs responsive to the catalysts.[33–36] To integrate the self-assembly of SPs with living cells, a biocompatible nucleophilic organocatalyst (2-(aminomethyl) benzimidazole derivative, **CAT**) was synthesized to replace traditionally used aniline or acid (Figure S2), which can also effectively catalyze hydrazone formation (Figure S3) thereon facilitate the self-assembly of **HA_3** (Figures S4 and S5). Furthermore, an aldehyde derivative bearing a single tail of oligomer ethylene glycol was used to enhance the self-assembly capability of the system (Figure 1a). The resulting monomers **HA_3** exhibit a critical assembly concentration (CAC) as low as ~10 μM (Figure S6), demonstrating a high self-assembly capability. Importantly, all the involved molecules are demonstrated to be nontoxic (Figure S2). By virtue of these features, we envision that the introduction of **CAT** into living cells would effectively accelerate the formation and self-assembly of **HA_3** inside the cells, thereby realizing intracellular production of the abiotic SPs (Figure 1d).

As the cellular internalization of **H** and **A** has been demonstrated in previous work,[31] therefore, to realize the intracellular self-assembly of the hydrazone-based SPs, the key lies in the successful loading of **CAT** in living cells. To investigate this, HeLa cells were incubated with 2 mM **CAT** for 4 h to allow for the internalization of **CAT** through the well-known passive diffusion mechanism.[37] By analyzing the cell lysates using high-performance liquid chromatography (HPLC), the presence of **CAT** was detected (Figure 2a), indicating the successful internalization of **CAT**. Furthermore, time-dependent measurements suggest that the cells complete internalization of **CAT** at 3 h, and the accumulated content of **CAT** increases from 0.5 to 4.0 μmol by enhancing the incubated [**CAT**] from 0.5 to 2.0 mM (Figure 2b, see Supporting Information). Unless stated otherwise, incubation of cells with 2.0 mM **CAT** for 4 h was used for the following studies to ensure a sufficient internalization of **CAT** for intracellular self-assembly.

Next, we are motivated to investigate whether the internalized **CAT** can accelerate the intracellular synthesis of the hydrazone-based SPs. For this purpose, the cells containing **CAT** were incubated with 0.45 mM **H** and 1.8 mM **A** for 4 h. Excess **A** was added to ensure a complete conversion of **H** into **HA_3**, and **H** was first reacted with 30 μM aldehyde-derived fluorescein (**A-FL**) before the incubation to visualize the self-assembled structures, (Figure S7).[38] After self-assembly, strong fluorescence is produced because of the condensation of the hydrazone-based monomers covalently decorated with fluorescein.[38] After incubation, all the samples were washed thoroughly with pure PBS to remove any unreacted molecules. Confocal microscopy observations show that, in contrast to the control sample without **CAT**, strong fluorescence is visible in the cells with **CAT** (Figure 2c), suggesting the occurrence of self-assembly. HPLC analysis confirmed that **HA_3** is formed in the cells (Figure S8). Moreover, the fluorescence intensity of the self-assembled objects is increased with the incubated [**H**] and [**CAT**] (Figures S9 and S10). To ensure the occurrence of self-assembly, the minimal [**H**] is ~0.15 mM with a [**CAT**] of 2.0 mM, while the minimal [**CAT**] is ~0.5 mM with a [**H**] of 0.45 mM. It should be noted that the cells incubated with pure **A-FL** have no fluorescence (Figure S11), further indicating that the observed fluorescence in the cells with **CAT** comes from the self-assembled objects rather than the intracellular accumulation of **A-FL**.

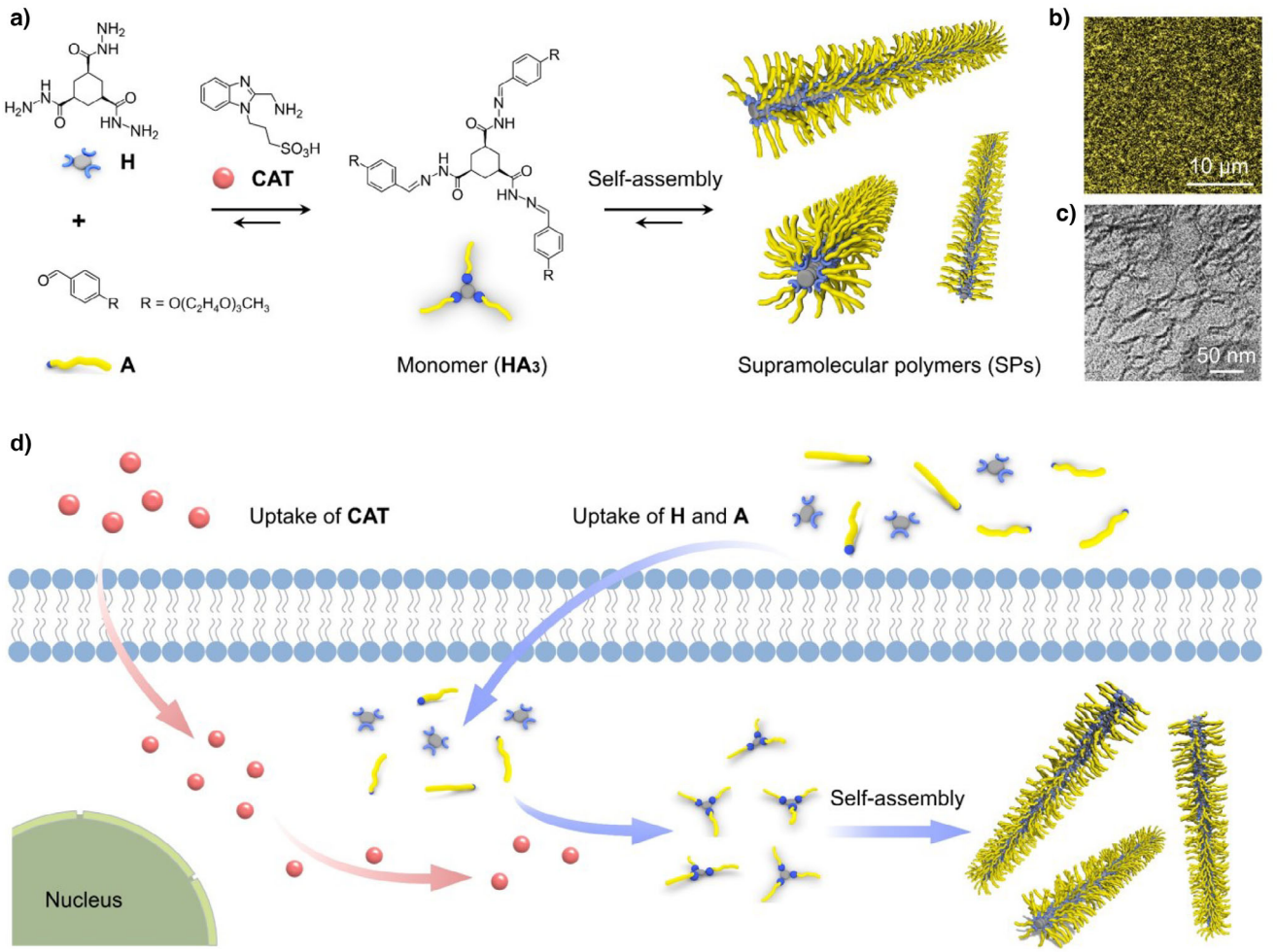

Figure 1. Conceptual illustration of the synthesis of abiotic SPs inside living cells. a) Formation of hydrazone-based monomers **HA_3** from non-assembling precursors **H** and **A** under the catalysis of 2-(Aminomethyl)benzimidazole derivative (**CAT**), and their subsequent self-assembly into SPs; b) confocal and c) TEM images showing the self-assembled SPs; d) scheme illustrating the intracellular production of the SPs relying on the organocatalysis-responsive self-assembly system by preinstalling the organocatalyst into cells. Samples: b, c) [**H**] = 10 mM, [**A**] = 40 mM, [**CAT**] = 10 mM in phosphate buffer (100 mM, pH 7.4).

To confirm the morphology of these self-assembled objects inside cells, transmission electron microscope (TEM) observations were performed. As shown in Figure 2d, clusters composed of short fibrous structures were observed in cells with **CAT** with respect to cells without **CAT**. Importantly, these short fibers have a diameter (d) of ~3.3 nm that is comparable to the hydrazone-based SPs (inset in Figure 2d). These TEM results together with the confocal observations confirm that the hydrazone-based SPs are produced inside the cells because of the intracellular organocatalysis effect. The limited length of the SPs in cells can be explained by their restricted growth in the crowded intracellular environment. It should be noted that although lysosome possesses an acidic environment, which may also catalyze hydrazone formation, the absence of any fluorescent objects in the control sample rules out lysosome-mediated intracellular self-assembly (Figure 2c). Due to the modular feature of the hydrazone-based SPs, various molecular functionalities like different fluorescence are allowed to be incorporated into the SPs (Figure S12), suggesting the high potential for functionalization of the SPs.

After demonstrating the synthesis of SPs inside the living cells, we are curious about the effects of these abiotic SPs on the physiological properties of cells. Because we expected that the growth of the SPs may destroy the subcellular structures, thus resulting in cell death,[39] we performed live-dead assays to examine the cell viability after growing the SPs. To our surprise, all the cells after growing the SPs with incubation [**CAT**] varying from 0 to 2 mM show a high viability of > 95% (Figure 3a and Figure S13). Furthermore, the proliferation ability of SPs-containing cells presents ignorable variations relative to the control group of SPs-free cells (Figure 3b). These results suggest that the formation of hydrazone and the SPs are compatible with the intracellular environment. Interestingly, we observed that the intracellular formation of SPs leads to a significant enlargement of the cell volume by around two times (Figure 3c and Figure S14), which can be attributed to the increased occupancy of cytoplasm space by

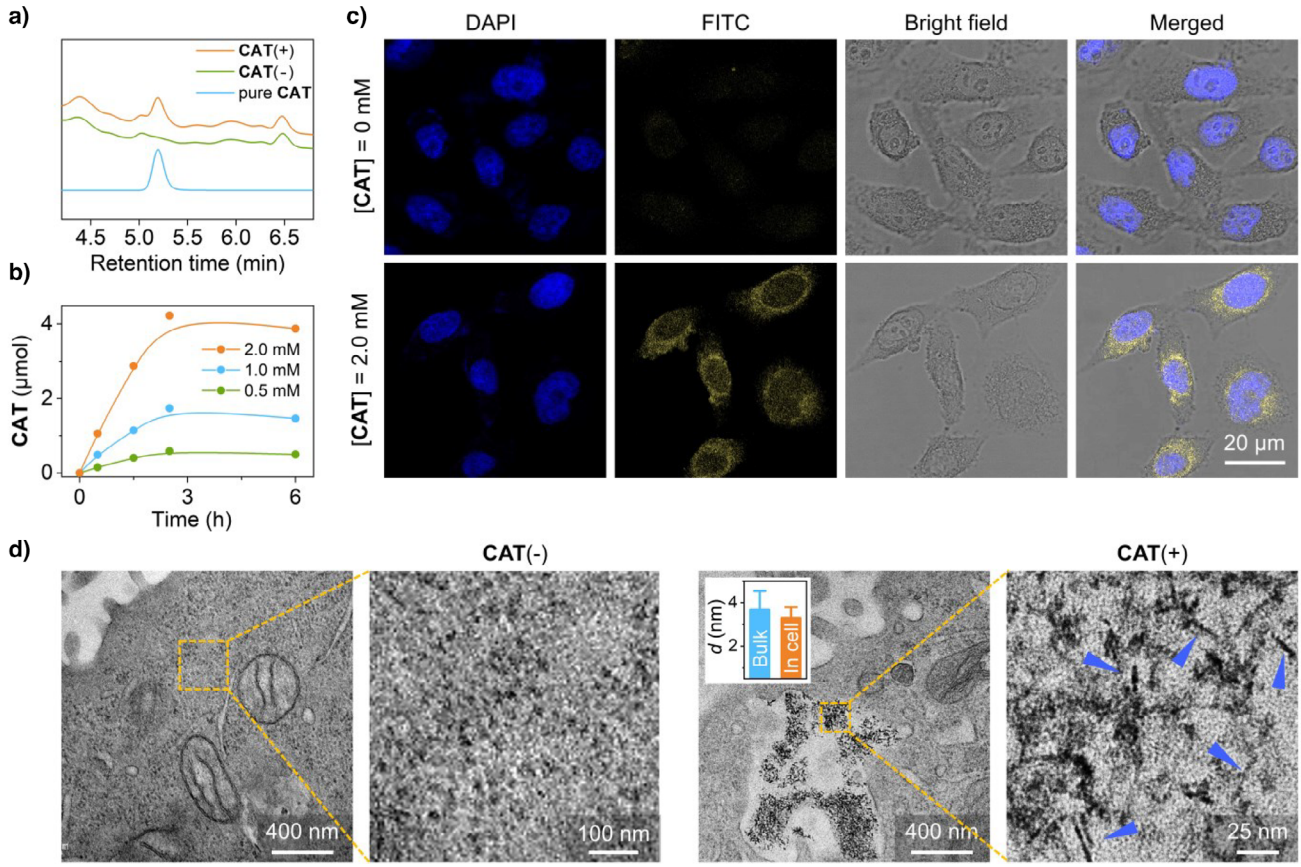

Figure 2. The internalization of **CAT** and in situ synthesis of hydrazone-based SPs in living cells. a) HPLC measurements demonstrating the internalization of **CAT** in the cells; and b) the content of **CAT** at varying incubation [**CAT**]; c) confocal images of the cells after incubations, FITC channel indicates the self-assembled structures inside the cells, and DAPI channel indicates the cell nucleus; d) TEM images showing the self-assembled objects in the samples of cell without **CAT**, **CAT**(-), and cell with **CAT**, **CAT**(+), the inset is the diameter (*d*) of the formed linear structures in bulk solution and cell, and the error bars are s.d. calculated from random 30 fibers. Samples: a) [**CAT**] = 2.0 mM; b) [**CAT**] = 0.5~2.0 mM; c,d) [**H**] = 0.45 mM, [**A**] = 1.8 mM, and [**CAT**] = 2 mM in phosphate buffer (100 mM, pH 7.4), [FITC] = 30 μM, [DAPI] = 20 μg mL^{-1}.

SPs. Yet the size of the nucleus remains the same, resulting in a significant reduction of the nucleus-to-cytoplasm (N/C) ratio (Figure 3c). We further found that, along with the cellular volume change, the stiffness of SPs-containing cells increased significantly (Figure S15), suggesting that the SPs have also impacted the cellular mechanics.

The intracellular formation of additional abiotic SPs may further enhance intracellular crowdedness, thereby slowing down intracellular diffusion, which possesses pivotal influences on many cell behaviors. To verify this, we probed the intracellular diffusion using the single quantum dot (QD) tracking technique.[40,41] The QDs were loaded into the cytosol and performed single-particle tracking of diffusing QDs at 33 Hz (Figure 3d and Movie S1). By analyzing the trajectories of QDs (Figure 3e), we determined the mean square displacement (MSD) and the diffusion coefficients (D) of the QDs. Our results show that the D in SPs-containing cells is reduced by 17% (Figure 3f), suggesting that the intracellular environment becomes more crowded. Furthermore, we analyzed the probability density function (PDF) of the QDs displacement (Figure 3g). Theoretically, diffusion in a homogeneous environment exhibits a Gaussian displacement distribution but deviates from Gaussian in a heterogeneous environment. We found that the SPs-containing cells show a more significant deviation from Gaussian, as quantified by the larger non-Gaussian parameters α_2 (Figure 3h), suggesting a more heterogeneous environment. These results indicate that the intracellular formation of the hydrazone-based SPs results in a more crowded and heterogeneous intracellular environment, in which the intracellular diffusion dynamics are slowed down.

It has been reported that intracellular diffusion dynamics and cell mechanical properties play crucial roles in cell migration behaviors.[42] In this context, we performed the live-cell long-term imaging of a single cell to monitor the cell migratory behavior (Figure 4a). Interestingly, we find that the cell trajectories of the SPs-containing cells are significantly shorter (Figure 4b and Movie S2). To quantify the trajectories, we further calculated the MSD_{cell} of cell trajectories and then determined the diffusion coefficients of the cell (D_{cell}) through the linear fitting of MSD using $MSD_{cell} = 4D_{cell}t + c$ (Figure 4c,d). The results of MSD_{cell} curves show that for the SPs-containing cells, the D_{cell} is 68% lower than for SPs-free cells. Consistent with the change in D_{cell}, the migration speed results also show that the intracellular formation of SPs reduces cell migration (Figure 4e). This observed hindered

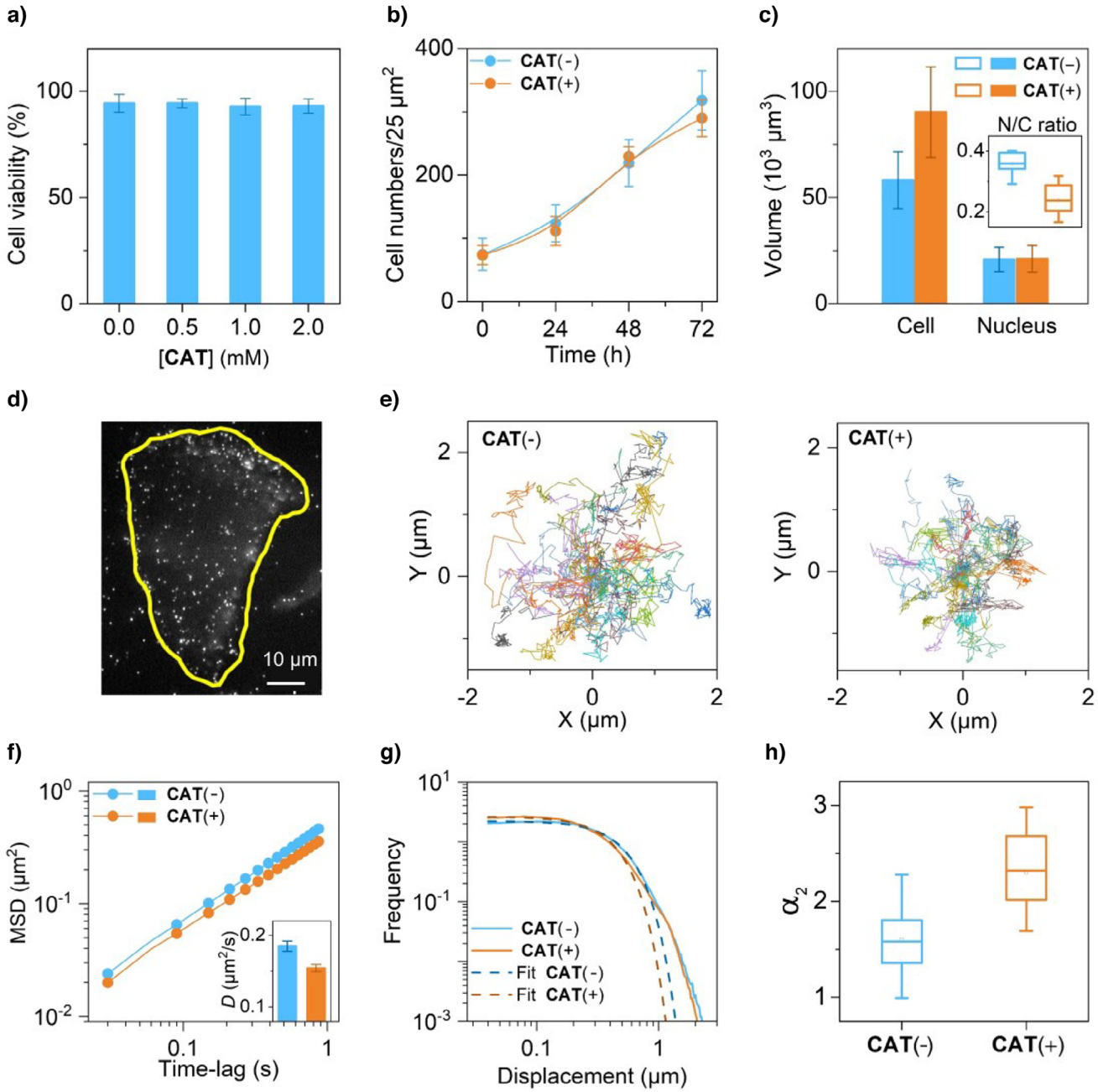

Figure 3. Effects of the hydrazone-based SPs on the physiological properties of cells in the cases of **CAT**(-) and **CAT**(+). a) The cell viability in the case of **CAT**(+) after treatment of 24 h measured by "live-dead" assay, the error bars are s.d. ($n = 3$); b) the cell proliferation ability of **CAT**(-) and **CAT**(+), the error bars are s.d. ($n = 5$); c) the cell volumes and nucleus volumes, inset is the corresponding N/C ratio of the cells, the error bars are s.d. ($n = 16$) and the differences between the distributions are significant at the $p < 0.001$ level; d) loading of QDs into cells for the analysis of intracellular diffusion; e) the QDs trajectories in the cells; f) the MSD from e), inset is the intracellular D, suggesting the reduced diffusion coefficient in **CAT**(+) group, the error bars are S.E.M. ($n = 28$); g) the PDF of the QD displacement; and h) non-Gaussian parameters α_2 demonstrating a more heterogeneous environment in **CAT**(+) group, the differences between the distributions are significant at the $p < 0.001$ level. Samples: a) [**H**] = 0.45 mM, [**A**] = 1.8 mM, and [**CAT**] = 0~2.0 mM in phosphate buffer (100 mM, pH 7.4); b–h) the **CAT**(+) group is [**H**] = 0.45 mM, [**A**] = 1.8 mM, and [**CAT**] = 2 mM in phosphate buffer (100 mM, pH 7.4).

cell migration in the presence of SPs can be attributed to the above-demonstrated restricted intracellular diffusion. Furthermore, from the nonlinear relationship of MSD_{cell} with time ($MSD_{cell} = A \times t^{\alpha}$), the exponent α provides the information of the motion modes, which indicates the directionality of cell migration. The SPs-containing cells show almost diffusive motion ($\alpha = 0.99 \pm 0.005$), while the SPs-free cells are superdiffusive motion ($\alpha = 1.06 \pm 0.01$) (Figure S16), suggesting that the SPs also weakened the directionality of cell migration.

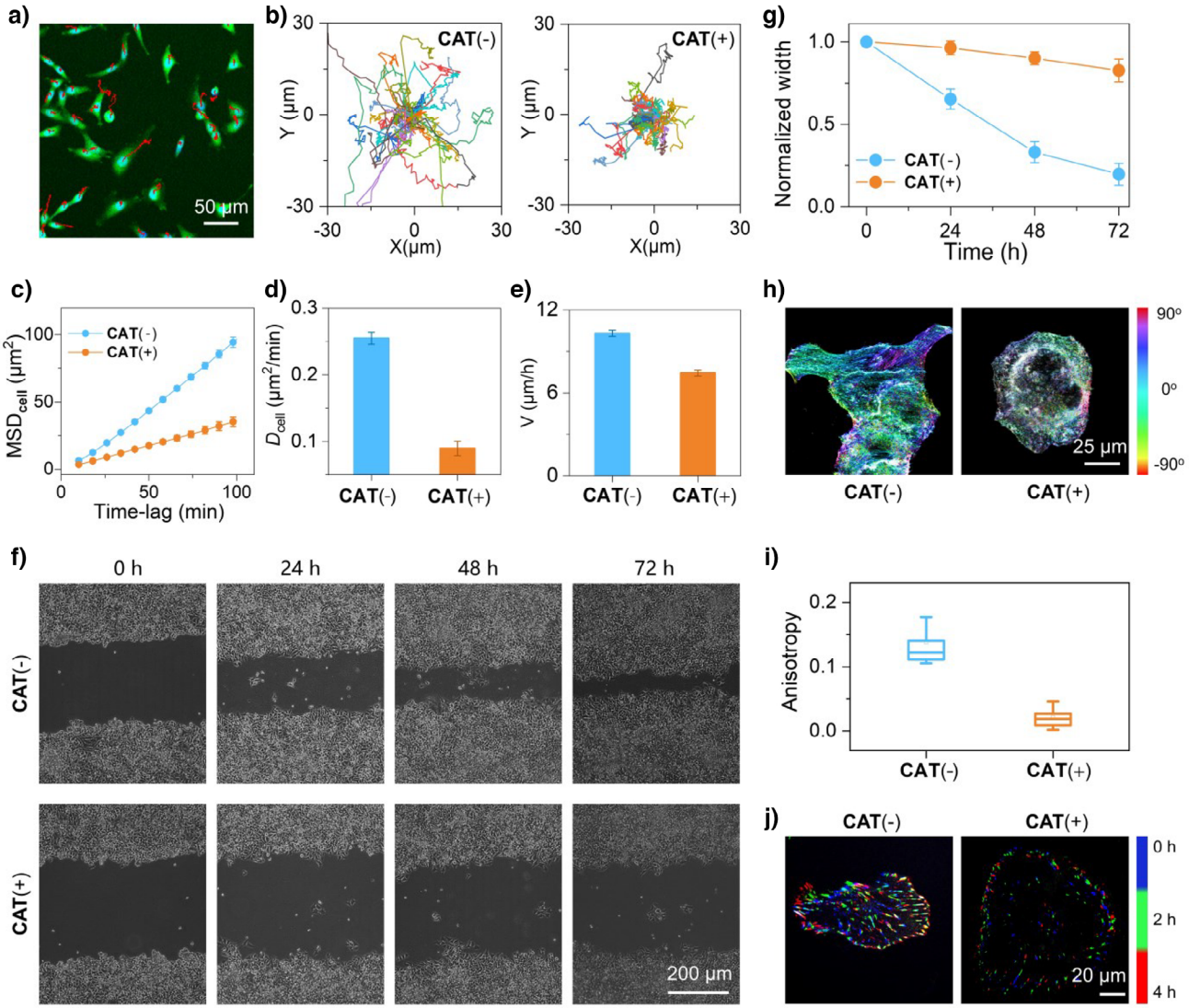

Figure 4. Influences of the hydrazone-based SPs on the cell migration behaviors. a) Scheme showing live-cell long-term imaging of a single cell; b) the cell trajectories of **CAT**(-) and **CAT**(+); c) MSD_{cell}, d) D_{cell} and, e) migration speed (V) of **CAT**(-) and **CAT**(+) showing the reduced cell migration with the intracellular formation of SPs, the error bars in c–e) are S.E.M. ($n = 400$); f) the wound-healing migration assay; and g) the corresponding normalized width of gap over time of **CAT**(-) and **CAT**(+), the error bars are s.d. ($n = 5$); h) confocal images showing the distribution of actin filaments in **CAT**(-) and **CAT**(+); and i) the corresponding anisotropy of the actin filaments analyzed by Image J, the differences batween the distributions are significant at the $p < 0.001$ level; and j) confocal images showing dynamic talins in **CAT**(-) and **CAT**(+) at different time points. Samples: b), f), h), and j) the **CAT**(+) group is [**H**] = 0.45 mM, [**A**] = 1.8 mM, and [**CAT**] = 2 mM in phosphate buffer (100 mM, pH 7.4), besides, h) [Phalloidin-FITC] = 5 μg mL^{-1}, and j) [Talin-GFP] = 5 mM for confocal measurements.

We further evaluated the influences of the in situ-formed SPs on the cell migration behaviors using wound-healing migration assays. The results show that the untreated cells and cells solely treated with **CAT** exhibit a significant migratory healing ability, with a high percentage of wound closure of >80% within 72 h after scratching (Figures S13 and S14). The cells incubated solely with **H** or **A** show relatively lower healing ability, but remain to have a percentage of wound closure of > 50% (Figures S17 and S18). However, in stark contrast, the SPs-containing cells sample with the formation of SPs shows a dramatically inhibited migratory healing ability, with a healing ratio of only 10% after 72 h (Figure 4f,g), in line with our results of the single-cell migratory behaviors.

As the intracellular formation of SPs increases the crowdedness inside the cells, it may interfere with the organization of actin filaments, which play key roles in cell migration.[43] To examine this, F-actin was stained with phalloidin-FITC to reveal the morphological changes in actin filaments after the formation of SPs (Figure 4h). We found that the actin filaments in the SPs-containing cells appeared to aggregate into locally disordered microdomains. As a comparison, the actin filaments in SPs-free cells are long-range and ordered fibrous structures. In addition, the actin orientation was also found to be altered. The anisotropy of the actin filaments in SPs-containing cells is significantly lower than SPs-free cells (Figure 4i). These results suggest that intracellular

polymerization of SPs interferes with the organization of actin filaments, which is also suggested to cause reduced cell motility. It should be noted that senescence-associated β-galactosidase (SA-β-Gal) staining suggests that the intracellular formation of SPs does not induce the aging effect on the cells (Figure S19).

Since actin filaments are closely associated with focal adhesions, which are crucial for cell migration, we further examined if the observed actin changes were accompanied by alterations in focal adhesions. As such, we fluorescently labeled talin with green fluorescent protein (GFP), which is a key component of focal adhesions. We transfected cells with talin-GFP and performed dynamic imaging of talin in migrating cells. We observed that talin became smaller and rounder in SPs-containing cells (Figure 4j). Moreover, from the merged talin images at different time points, we found that there was less overlap in SPs-containing cells compared with the control sample (Figure 4j and Movie S3), suggesting that the focal adhesions in SPs-containing cells have a shorter lifetime. Collectively, the smaller and less stable focal adhesions we observed in SPs-containing cells further confirmed the inhibition effect of the intracellularly formed SPs on cell migration.

Conclusion

In this study, we have demonstrated the synthesis of fully abiotic hydrazone-based SPs inside living cells using an organocatalysis-mediated self-assembly strategy, and the in situ-generated SPs restrict cellular motility. By incorporating an organocatalyst into cells, synthetic precursors of hydrazide and aldehyde are converted into hydrazone-based monomers that are capable of self-assembling into SPs within the highly complex intracellular environment. Interestingly, the in situ-formed SPs exhibit negligible effects on cell viability and proliferation but change psychological properties, such as cell volumes and stiffness. Importantly, the cells with in situ-generated SPs are found to show hindered migratory ability, which seems to be a result of the restricted intracellular diffusion and changes in the organization of the actin cytoskeleton. Such a hindered migration effect of SPs shows potent potential to impede the migration and invasion of cancer cells.

It is believed that immense small molecular building blocks can be designed and synthesized, which are allowed to easily enter cells through passive diffusion and assemble into functionalized SPs inside cells. These in situ-generated SPs are expected to reinforce the inherent cellular functions or even enable completely new functions to living systems; therefore, bridging the gap between synthetic chemistry and the living realm. In the next step, the organocatalysts can be designed to target cancer cells or specific regions in cells such that the SPs can be spatially triggered to form at the areas of interest for functions. Moreover, new monomers with sufficiently lower CAC can be designed, for instance, by enhancing the intermolecular interactions, to accelerate down-to-earth biological applications. Furthermore, the SPs can be decorated with drugs to serve as intracellular drug reservoirs to enhance anticancer efficacies, especially for cancer cells with drug resistance.

Supporting Information

Materials, instrumentations and experimental sections.

Movie S1. Intracellular diffusion of QDs in the samples of **CAT**(−) and **CAT**(+).

Movie S2. Cell migration in the samples of **CAT**(−) and **CAT**(+).

Movie S3. Intracellular movement of talin in the samples of **CAT**(−) and **CAT**(+).

Acknowledgements

Y.W. acknowledges the financial support of the Natural Science Foundation of Shanghai (22ZR1417700), Shanghai Pilot Program for Basic Research (22TQ1400100-9), NSFC (21908061), the "Chenguang Program" supported by the Shanghai Education Development Foundation and Shanghai Municipal Education Commission (20CG36), and National Key Research and Development Program of China (2022YFD70050101). H.L. acknowledges the financial support from National Natural Science Foundation of China (12122402), and the Fundamental Research Funds for the Central Universities. The authors acknowledge Mr. Yunfei Xu from Hangzhou Surface Power Technology Co., Ltd. for the cytomechanics measurement using the Piuma Nanoindenter (Optics11 Life, Netherlands).

Conflict of Interests

The authors declare no conflict of interest.

Data Availability Statement

The data that support the findings of this study are available in the supplementary material of this article.

Keywords: Gelation · Intracellular self-assembly · Local catalysis · Supramolecular polymers

[1] P. T. Conduit, A. Wainman, J. W. Raff, *Nat. Rev. Mol. Cell. Biol.* **2015**, *16*, 611–624.
[2] N. Ofera, A. Mogilner, K. Keren, *Proc. Natl. Acad. Sci. U.S.A.* **2011**, *108*, 20394–20399.
[3] P. R. Clarke, *Science* **2005**, *309*, 1334–1335.
[4] A. Agrawal, Z. C. Scott, E. F. Koslover, *Annu. Rev. Biophys.* **2022**, *51*, 247–266.
[5] N. B. Gudimchuk, J. R. McIntosh, *Nat. Rev. Mol. Cell. Bio.* **2021**, *22*, 777–795.
[6] A. Zhang, S. Zhao, J. Tyson, K. Deisseroth, Z. Bao, *Nat. Synth.* **2024**, *3*, 943–957.

[7] H. He, W. Tan, J. Guo, M. Yi, A. N. Shy, B. Xu, *Chem. Rev.* **2020**, *120*, 9994–10078.
[8] Q. X. Zhang, W. Y. Tan, Z. Y. Liu, Y. C. Zhang, W. S. Wei, S. Fraden, B. Xu, *J. Am. Chem. Soc.* **2024**, *146*, 12901–12906.
[9] C. Liu, H. Ma, S. Yuan, Y. Jin, W. Tian, *ACS Nano* **2025**, *19*, 2047–2069.
[10] H. Wang, Y. Q. Song, W. S. Wang, N. L. Chen, B. B. Hu, X. Liu, Z. Y. Zhang, Z. L. Yu, *J. Am. Chem. Soc.* **2024**, *146*, 330–341.
[11] M. H. Yi, Z. Q. Q. Feng, H. J. He, D. Dinulescu, B. Xu, *J. Med. Chem.* **2023**, *66*, 10027–10035.
[12] Z. Feng, H. Wang, X. Chen, B. Xu, *J. Am. Chem. Soc.* **2017**, *139*, 15377–15384.
[13] C. Wu, C. L. Wang, Y. Y. Zheng, Y. X. Zheng, Z. Q. Liu, K. M. Xu, W. Y. Zhong, *Adv. Funct. Mater.* **2021**, *31*, 2104418.
[14] Z. H. Di, X. L. Yi, L. L. Li, *J. Am. Chem. Soc.* **2023**, *145*, 7931–7940.
[15] N. L. Chen, Z. Y. Zhang, X. Liu, H. B. Wang, R. C. Guo, H. Wang, B. B. Hu, Y. Shi, P. Zhang, Z. H. Liu, Z. L. Yu, *J. Am. Chem. Soc.* **2024**, *146*, 10753–10766.
[16] F. Tian, R. C. Guo, C. X. Wu, X. Liu, Z. Y. Zhang, Y. M. Wang, H. Wang, G. Y. Li, Z. L. Yu, *Angew. Chem. Int. Ed.* **2024**, *63*, e202404703.
[17] Z. Y. Liu, J. Q. Guo, Y. C. Qiao, B. Xu, *Acc. Chem. Res.* **2023**, *56*, 3076–3088.
[18] W. M. Xiong, N. Song, X. W. Mo, Z. Y. Zhang, J. Y. Song, Y. S. Wang, J. Y. Li, Z. L. Yu, *Chem. Rev.* **2025**, *523*, 216251.
[19] R. Wang, L. Zhou, Y. Y. Yang, F. R. Zhao, X. B. Sun, X. Y. Liu, Z. Zou, G. L. Liang, *J. Am. Chem. Soc.* **2024**, *146*, 34870–34877.
[20] H. Yin, Y. Hua, S. W. Feng, Y. Xu, Y. Ding, S. C. Liu, D. S. Chen, F. R. Du, G. L. Liang, W. J. Zhan, Y. Shen, *Adv. Mater.* **2024**, *36*, 2308504.
[21] S. Sun, H. W. Liang, H. Wang, Q. M. Zou, *ACS Nano* **2022**, *16*, 18978–18989.
[22] T. Ma, R. Chen, N. Lv, Y. Li, Z. R. Yang, H. Qin, Z. Li, H. Jiang, J. Zhu, *SmallSmall* **2022**, *18*, 2204759.
[23] J. Geng, W. S. Li, Y. C. Zhang, N. Thottappillil, J. Clavadetscher, A. Lilienkampf, M. Bradley, *Nat. Chem.* **2019**, *11*, 578–586.
[24] Q. Shen, Y. Huang, Y. Zeng, E. Zhang, F. T. Lv, L. Liu, S. Wang, *ACS Mater. Lett.* **2021**, *3*, 1307–1314.
[25] Y. Zhang, Q. Gao, W. S. Li, R. K. He, L. W. Zhu, Q. J. Lian, L. Wang, Y. Li, M. Bradley, J. Geng, *J. Am. Chem. Soc. Au* **2022**, *2*, 579–589.
[26] Y. Dai, T. Li, Z. Zhang, Y. Tan, S. Pan, L. Zhang, H. Xu, *J. Am. Chem. Soc.* **2021**, *143*, 10709–10717.
[27] L. L. Li, S. L. Qiao, W. J. Liu, Y. Ma, D. Wan, J. Pan, H. Wang, *Nat. Commun.* **2017**, *8*, 1276.
[28] L. Cui, S. Vivona, B. R. Smith, S. R. Kothapalli, J. Liu, X. Ma, Z. Chen, M. Taylor, P. H. Kierstead, J. M. J. Fréchet, S. S. Gambhir, J. Rao, *J. Am. Chem. Soc.* **2020**, *142*, 15575–15584.
[29] S. Kim, B. Jana, E. M. Go, J. E. Lee, S. Jin, E. K. An, J. Hwang, Y. Sim, S. Son, D. Kim, C. Kim, J. Jin, S. K. Kwak, J. H. Ryu, *ACS Nano* **2021**, *15*, 14492–14508.
[30] K. Y. Zhang, Q. Feng, Z. W. Fang, L. Gu, L. M. Bian, *Chem. Rev.* **2021**, *121*, 11149–11193.
[31] F. Versluis, D. M. van Elsland, S. Mytnyk, D. L. Perrier, F. Trausel, J. M. Poolman, C. Maity, V. A. A. le Sage, S. I. van Kasteren, J. H. van Esch, R. Eelkema, *J. Am. Chem. Soc.* **2016**, *138*, 8670–8673.
[32] J. Boekhoven, J. M. Poolman, C. Maity, F. Li, L. van der Mee, C. B. Minkenberg, E. Mendes, J. H. van Esch, R. Eelkema, *Nat. Chem.* **2013**, *5*, 433–437.
[33] A. G. L. Olive, N. H. Abdullah, I. Ziemecka, E. Mendes, R. Eelkema, J. H. van Esch, *Angew. Chem. Int. Ed.* **2014**, *53*, 4132–4136.
[34] C. Maity, W. E. Hendriksen, J. H. van Esch, R. Eelkema, *Angew. Chem. Int. Ed.* **2015**, *54*, 998–1001.
[35] Y. M. Wang, F. Versluis, S. Oldenhof, V. Lakshminarayanan, K. Zhang, Y. W. Wang, J. Wang, R. Eelkema, X. H. Guo, J. H. van Esch, *Adv. Mater.* **2018**, *30*, 1707408.
[36] Y. M. Wang, S. Oldenhof, F. Versluis, M. Shah, K. Zhang, V. van Steijn, X. H. Guo, R. Eelkema, J. H. van Esch, *Small* **2019**, *15*, 1804154.
[37] J. Mosquera, I. García, L. M. Liz-Marzán, *Acc. Chem. Res.* **2018**, *51*, 2305–2313.
[38] Y. M. Wang, M. Lovrak, Q. Liu, C. Maity, V. A. A. le Sage, X. H. Guo, R. Eelkema, J. H. van Esch, *J. Am. Chem. Soc.* **2019**, *141*, 2847–2851.
[39] J. Li, Y. Kuang, J. F. Shi, J. Zhou, J. E. Medina, R. Zhou, D. Yuan, C. H. Yang, H. M. Wang, Z. M. Yang, J. F. Liu, D. M. Dinulescu, B. Xu, *Angew. Chem. Int. Ed.* **2015**, *54*, 13307–13311.
[40] H. Li, S. X. Dou, Y. R. Liu, W. Li, P. Xie, W. C. Wang, P. Y. Wang, *J. Am. Chem. Soc.* **2015**, *137*, 436–444.
[41] M. L. Zhang, Z. H. Zhang, X. Z. Niu, H. Y. Ti, Y. X. Zhou, B. Gao, Y. W. Li, J. L. Liu, X. S. Chen, H. Li, *Adv. Sci.* **2024**, *11*, 2308338.
[42] C. Jiang, H. Y. Luo, X. P. Xu, S. X. Dou, W. Li, D. S. Guan, F. F. Ye, X. S. Chen, M. Guo, P. Y. Wang, H. Li, *Nat. Commun.* **2023**, *14*, 5166.
[43] L. J. Macdougall, T. E. Hoffman, B. E. Kirkpatrick, B. D. Fairbanks, C. N. Bowman, S. L. Spencer, K. S. Anseth, *Adv. Mater.* **2022**, *34*, 2202882.

Manuscript received: January 13, 2025
Revised manuscript received: March 07, 2025
Accepted manuscript online: March 09, 2025
Version of record online: March 17, 2025